The effect of different particle residence time distributions on the chemical looping combustion process

Journal Article

Author(s):
Schnellmann, Matthias A.; Donat, Felix; Scott, Stuart A.; Williams, Gareth; Dennis, John S.
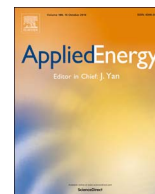
The effect of different particle residence time distributions on the chemical looping combustion process

Matthias A. Schnellmann[a,*], Felix Donat[b], Stuart A. Scott[c], Gareth Williams[d], John S. Dennis[a]

[a] Department of Chemical Engineering & Biotechnology, University of Cambridge, Pembroke Street, Cambridge CB2 3RA, United Kingdom
[b] Institute of Energy Technology, ETH Zürich, Leonhardstrasse 21, LEE P225, 8092 Zürich, Switzerland
[c] Department of Engineering, University of Cambridge, Trumpington Street, Cambridge CB2 1PZ, United Kingdom
[d] Johnson Matthey Technology Centre, Blounts Court Road, Sonning Common, Reading RG4 9NH, United Kingdom

HIGHLIGHTS

- Model for a reactor-regenerator system has been developed.
- Residence time distribution of solids is important in chemical looping combustion.
- Reducing the extent of solid mixing increases the extent of conversion and rates.
- Residence time distribution of solids should be accounted for in simulations.

ARTICLE INFO

ABSTRACT

A model for chemical looping combustion has been developed to allow the effect of different residence time distributions of oxygen carrier particles in the air and fuel reactors to be investigated. The model envisages two, coupled fluidised bed reactors with steady circulation of particles between them. The results show that the process is sensitive to the residence time distributions, particularly when the mean residence time of particles in the reactors is similar to the time required for them to react completely. Under certain operating conditions, decreasing the variance of the residence time distribution, leads to a greater mean conversion of the particles by the time they leave the reactors and higher mean rates of reaction in the beds. In this way the required inventory and circulation rate of solids could be reduced, which would lower the capital and operating costs of a CLC process. Since the residence time distribution of solids is important, it should be taken into account when modelling or designing a chemical looping combustion process, *e.g.* by using a tanks-in-series model. This work indicates that if the number of tanks, $N \leq 5$, knowing N to the nearest integer is generally sufficient, unless a high degree of accuracy is needed. As N increases, the sensitivity of the coupled system decreases, so for $N > 5$, knowing the value to the nearest 5 or 10 tanks is sufficient. This is valid whether N is the same or different in the two reactors. Chemical looping combustion is one example of a reactor-regenerator system, so the results are also relevant for other processes of this type, such as fluidised catalytic cracking.

1. Introduction

Chemical looping combustion (CLC) is a technique which allows fossil fuels to be burnt with inherent capture of the carbon dioxide emissions. It is based on the redox cycling of an oxygen carrier, which is typically an oxide of a transition metal. The carrier supplies oxygen from its crystal lattice in the fuel reactor and is reduced in the process. It is then transferred to the air reactor where the oxide is regenerated by reaction with air. CLC is thus a type of reactor-regenerator system, often exemplified by fluidised catalytic cracking [1]. Generally CLC is

designed in a configuration consisting of two interconnected fluidised bed reactors [2,3], as shown in Fig. 1. Reduction of the oxygen carrier takes place in the fuel reactor, while regeneration is conducted in the air reactor.

A significant amount of research has been conducted on CLC, ranging from the scale of the oxygen carrier materials [2,4] up to the industrial scale, such as modelling the integration of CLC reactors with a power cycle for generating electricity [5]. At the scale of the interconnected fluidised bed reactors, a number of different pilot scale units have been built and operated with a variety of different oxygen carrier
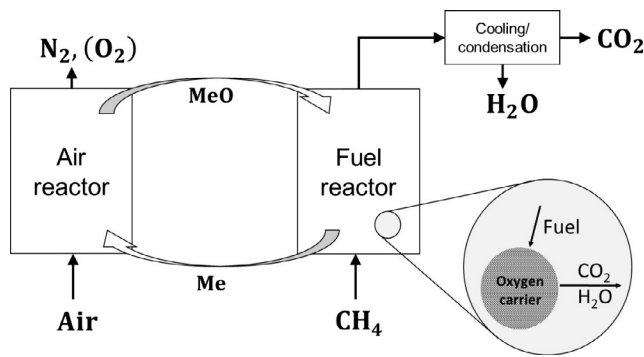
Fig. 1. The CLC process. Me is an appropriate transition metal.

materials and fuels up to 3 MWth [6–9]. Modelling of such reactors has also been conducted, ranging from empirical [10] or semi-empirical [11] to CFD [12–15]. Virtually all modelling has been applied to particular reactor designs, oxygen carrier materials and fuels, which has enabled certain aspects of these configurations to be evaluated. For example Cuadrat et al. [16] optimised different conditions such as the carbon separations system, the fuel reactor temperature and the solids inventory for an iG-CLC system for solid fuels with ilmenite as oxygen carrier. Zhang et al. [17] modelled an interconnected double loop circulating fluidised bed and analysed the influence of different operating conditions such as the temperature of the fuel reactor and the fuel power on its performance. Ohlemüller et al. [18] developed a process model for CLC with coal in a 100kWth system. They used it to study the effect of factors such as pressure drop, temperature and solid circulation on the performance of the pilot unit. A general CLC process and its sensitivity to different factors has rarely been considered. This would be valuable for reverse engineering an optimal process and also for developing computationally-efficient and accurate simulations by accounting for each factor at the right level of detail.

In this paper, a model that is general to any CLC process is used to investigate the effect of different residence time distributions (RTDs) of particles on its performance. This has received little attention in the literature on CLC or reactor-regenerator systems. It is important since the RTD is well-known to significantly influence the performance of reactors [19] and understanding these effects would allow the CLC process to be optimised, as will be demonstrated in this paper. Further, it gives insight for developing computationally-efficient and accurate simulations of the CLC process. Particularly for solid systems, RTDs are time-consuming, expensive and challenging to determine, irrespective of whether the laboratory or the industrial scale is being considered. Accordingly, experimental RTDs from a laboratory-scale circulating fluidised bed (CFB) have been used in this paper to understand how detailed an experimental determination of the RTDs of a real system must be to give useful information.

1.1. The residence time distribution function

The RTD of material in a system can be represented by the RTD function, $E(t)$, which gives the distribution of times that material spends in a system. $E(t)dt$ is the fraction of material spending a time between t and $t + dt$ in the reactor. Therefore [19]:

$$\int_0^\infty E(t)dt = 1 \tag{1}$$

The mean residence time, $\bar{t}$ is given by:

$$\bar{t} = \int_0^\infty tE(t)dt \tag{2}$$

and the variance, σ^2 by:

$$\sigma^2 = \int_0^\infty (t-\bar{t})^2 E(t)dt \tag{3}$$

In general, the solids in fluidised beds are assumed to be well-mixed [19–23]. As a result, a tanks-in-series (TIS) model is often used to represent the RTD function [24–28], where it is assumed that the system consists of N continuous stirred tank reactors (CSTRs), of equal volume, in series. Each tank is statistically independent and, in each, the solids are perfectly mixed. The RTD is given by [29]:

$$E(t) = \frac{t^{N-1}}{\bar{t}^N} \frac{N^N}{(N-1)!} e^{-\frac{Nt}{\bar{t}}} \tag{4}$$

where t is the time a particle spends in the overall reactor. $N = 1$ corresponds to a well-mixed system and as $N \to \infty$, the RTD from the model approaches plug flow. The variance, σ^2, of the RTD is

$$\sigma^2 = \frac{\bar{t}^2}{N} \tag{5}$$

In this form, the TIS model is only valid for $N \in \mathbb{N}$. The model can be adapted so that N can take non-integer values e.g. the fractional tank model [29] or the gamma extension model [30]. In the gamma extension model, the gamma function, $\Gamma(N)$ is used as a generalised factorial function and replaces the $(N-1)!$ term in Eq. (4):

$$\Gamma(N) = \int_{x=0}^\infty e^{-x} x^{N-1} dx \tag{6}$$

where N can now be any rational number greater than zero.

2. Model development

The model developed in this work was based on two, coupled fluidised bed reactors, with steady circulation of particles between them, as depicted in Fig. 1. In terms of the gas-solid reaction, a characteristic time for a particle to react completely in the air and in the fuel reactor, $t_{tot,air}$ and $t_{tot,fuel}$ respectively was specified. These two parameters were inputs to particle models, describing the rate of reaction of oxygen carrier particles, assumed to be either shrinking core (controlled by one or more of intrinsic chemical reaction, diffusion through the product layer and external mass transfer) or uniform throughout the particle [31]. In this paper, which is general for any CLC system, a non-dimensional time, θ was used throughout, where

$$\theta = \frac{t_{tot}}{\bar{t}} \tag{7}$$

and $\bar{t}$ is the mean residence time of particles in the air or the fuel reactor. Large values of θ correspond to short residence times and small values to long residence times compared to the time taken for a particle to react completely. A non-dimensional time was used to make the model general to any CLC system, regardless of the scale. In fact it is general to any reactor-regenerator system. It also meant that it was not necessary to have precise values for $t_{tot,air}$ and $t_{tot,fuel}$.

The RTD of the particles in the reactors was modelled using a tanks-in-series (TIS) model, where N can take non-integer values (Eqs. (4) and (6)). The particles were assumed to be of equal size and it was assumed that there was no irreversible decay in performance over time. The latter is an appropriate assumption to make since the time taken for the CLC process to reach a steady state would usually be short compared to the time taken for the performance of particles to deteriorate due to repetitive redox cycling. The state of conversion of particles was tracked over time. This is important since particles can build up complex local distributions of oxidised and reduced material as they are cycled between the air and fuel reactors [32].

A Monte Carlo (MC) approach was used to determine the mean conversion of the stream of particles as they leave the air and the fuel reactors, X_{air} and X_{fuel} respectively. The mean rates of reaction of particles within the beds were also determined. When the system is well mixed ($N = 1$), the properties of the particles within the bed are the same as the properties of the particles leaving the bed. In all other cases, there is a difference, which reaches a maximum as plug flow is

approached ($N \gg 1$). In the MC simulation, a single particle was cycled at least 1000 times with different values of θ.

The particle being cycled carries the complete statistics of the process. When simulating steady state behaviour, these statistics remain constant over time. The ergodic hypothesis can therefore be invoked, stating that cycling one particle x times gives the same distribution of values as cycling x particles once. The initial conversion does not matter since after a small number of cycles, it becomes insignificant. From the second time that the particle enters a reactor, its initial conversion is the final conversion with which it left the other reactor *i.e.* the initial conditions are automatically determined. Each time the particle entered a reactor, the time that it spent there was determined using a rejection sampling algorithm from the appropriate RTD. The modelling approach was similar to that used by Schnellmann et al. [31].

The modelling approach could be applied to a specific CLC system to evaluate further aspects, such as the conversion of the fuel in the fuel reactor. This is beyond the scope of this paper. It could be done by refining the particle model and determining precise times for particles to react completely experimentally. The experiments should use the chosen oxygen carrier material and fuel and the conditions should replicate those that the particles would experience in the two reactors in the specific CLC system *e.g.* temperature and gas concentrations.

3. Results

3.1. Sensitivity of CLC to the RTD functions of particles in the air and fuel reactors

A number of MC simulations were run, using the TIS model (Eqs. (4) and (6)) for the RTDs of the oxygen carrier particles. Values of N, ranging from 1 to 50, were used to account for the full range of possible RTDs from well-mixed to approaching the plug flow limit, as shown in Fig. 2. The results of these simulations are shown in Figs. 3–6. For the case where the oxygen carrier particles were well mixed, the analytical solution rather than the MC result is shown [32], there being excellent agreement between the analytical solution and the MC result [31]. By accounting for the range of possible RTDs, Fig. 3 shows the envelope of possible mean conversions that particles can have when leaving the air and fuel reactors for different values of θ. Throughout this paper, results are shown for the case where the particles react according to a shrinking core model under chemical reaction control. The trends for the other forms of kinetics, described in Section 2 were similar.

From Fig. 3, it is clear that for $\theta > 0.1$, if the RTD is changed, it has an impact on the mean conversion of particles as they leave the reactors. The sensitivity reaches a peak when θ is between 1 and 2. This corresponds to the operating region where the mean residence time is similar to the time taken for a particle to react completely. If θ is kept
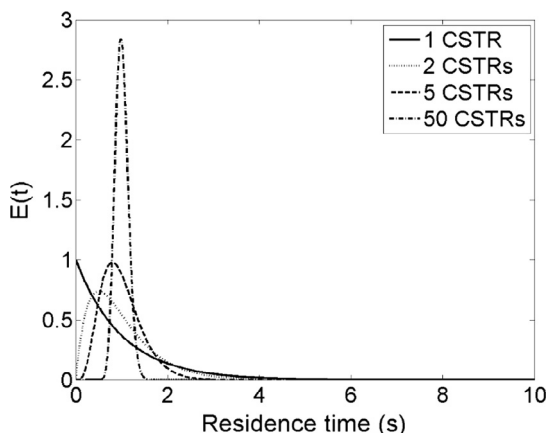

Fig. 2. The RTDs used to explore the sensitivity of the CLC process. The RTDs are all plotted with a mean residence time of 1 s.
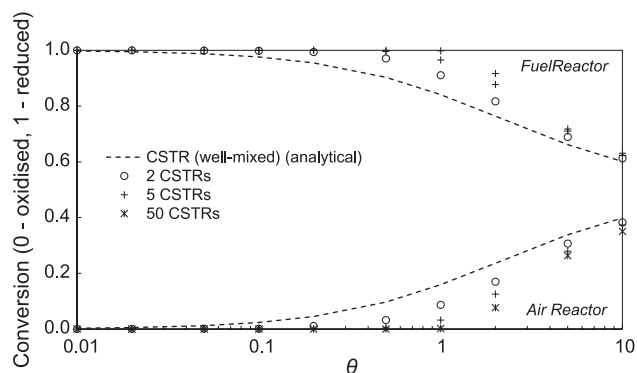

Fig. 3. Mean conversion of particles as they leave the reactors for different RTDs.
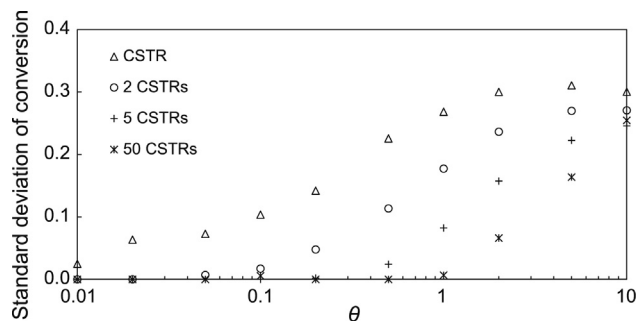

Fig. 4. Standard deviation of conversion of particles as they leave the reactors for different RTDs. The fuel reactor results are shown. The air reactor results have the same form since a non-dimensional time, θ, has been used.
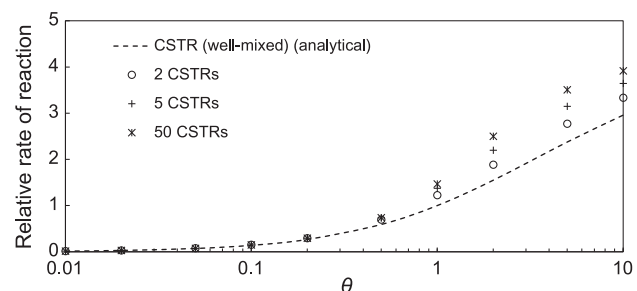

Fig. 5. Mean rate of reaction of particles in the beds for different RTDs. The fuel reactor results are shown. The air reactor results have the same form since a non-dimensional time, θ, has been used and the rates are relative to the well-mixed value when $\theta = 1$.
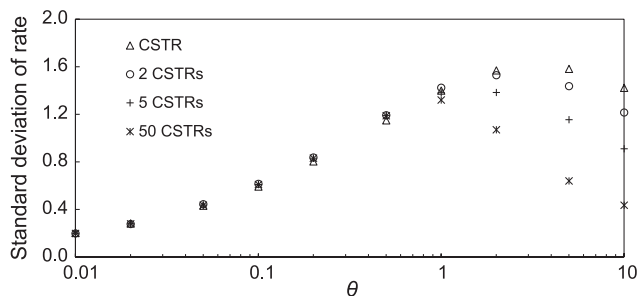
Fig. 6. Standard deviation of rate of reaction of particles in the beds for different RTDs. The fuel reactor results are shown. The air reactor results have the same form since a non-dimensional time, θ, has been used and the rates are relative to the well-mixed value when $\theta = 1$.

constant, a decrease in the extent of mixing leads to a greater $\Delta X = X_{fuel} - X_{air}$, *e.g.* if $\theta = 1$, an increase in the value of N in both reactors from 1 to 2 gives an increase in ΔX from 0.682 to 0.824. Therefore the same amount of oxygen can be transferred between the

air and the fuel reactor but at a reduced solid circulation rate.

Fig. 4 shows the variation in the standard deviation of the conversion of particles as they leave the reactors, for different RTDs. As expected, it can be seen that a greater degree of mixing leads to a larger standard deviation. In the plug flow limit ($N = 50$), for $\theta < 1$, there is almost no spread since the particles leave the reactors completely oxidized or reduced. A standard deviation of 0 is only achieved for $\theta > 1$ when there is perfect plug flow.

Fig. 5 shows how the mean rate of reaction of particles in the beds varies for different RTDs. For simplicity and so that the air and fuel reactor results are the same, the mean rate of reaction is shown relative to the well-mixed value when $\theta = 1$. When operating in a regime where $\theta > 0.5$ in the reactors, the mean rate of reaction is sensitive to different RTDs. The rate of reaction is higher when there is less mixing, which agrees with the higher mean conversion of particles as they leave the reactors seen in Fig. 3.

Fig. 6 shows the sensitivity of the standard deviation of the rate of reaction of particles in the reactors for different RTDs. For $\theta < 0.5$, the standard deviations are the same, irrespective of the RTD. At larger values of θ, the values diverge, with a well-mixed system exhibiting a greater spread of rate of reaction.

The values of ΔX between the exit streams of the reactors and the mean rates of reaction in the reactors, were used to determine the circulation rate of solids, $\dot{m}_s$ and the inventories of solids, m_{fuel} and m_{air}, required of the CLC system. Thus,

$$\dot{m}_s = \frac{2af}{\rho_m \Delta X} \tag{8}$$

$$m_{fuel} = \frac{f}{r_{fuel}} \tag{9}$$

$$m_{air} = \frac{af}{r_{air}} \tag{10}$$

where a is a stoichiometric coefficient (moles O_2/mole fuel), f is the flow rate of fuel (moles fuel/s), ρ_m is a molar density of the oxygen carrier (moles lattice O/g carrier) and r_{fuel} (mol fuel/s/g carrier) and r_{air} (mol O_2/s/g carrier) are the mean rates of reaction in the fuel and air reactors respectively. The results are shown in Fig. 7. Both the circulation rate and the inventories are given relative to the well mixed values when $\theta = 1$.

The lowest circulation rate is achieved when $\Delta X = 1$, which is the case when the particles are given sufficient time to react completely, i.e. when CLC is operated with low values of θ. As the RTD tends toward the plug flow limit, the value of θ necessary to achieve $\Delta X = 1$ tends to unity. On the other hand, in order to reduce the inventories in the air and fuel reactors, a high rate of reaction in the beds and therefore operation with high values of θ is desirable. As the RTD tends toward plug flow, it leads to lower inventories.
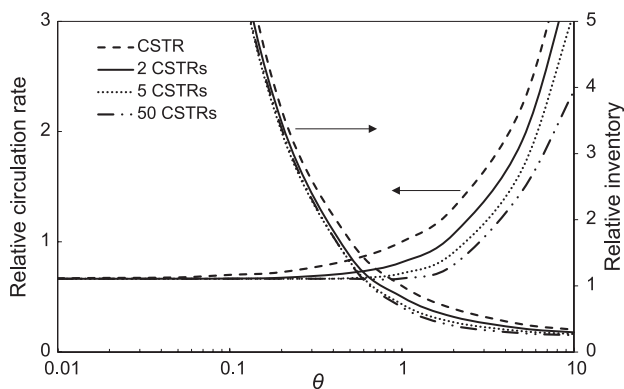

Fig. 7. Circulation rate and inventory of CLC for different RTDs. Both the circulation rate and the inventory are relative to the well-mixed value when $\theta = 1$.

3.2. Experimental RTDs of particles

Donat [14] measured the RTDs of particles for the air and fuel reactors in a laboratory-scale circulating fluidised bed (CFB) at room temperature. Silica sand particles were used, sieved to 180–250 µm. The particle density, ρ_p was 2650 kg/m^3, the minimum fluidisation velocity, U_{mf} was 0.0485 m/s and the bed voidage at U_{mf}, ε_{mf} was 0.465. The total inventory of particles was ~ 0.4 kg. The CFB was operated under ambient conditions, with $U_0/U_{mf} = 6$ and $U_0/U_{mf} = 2.2$ in the air and fuel reactors, respectively, where U_0 is the superficial fluidising velocity. A description of the apparatus is given in Appendix A and further information is given by Donat et al. [33]. While the CFB was in operation, positron emission particle tracking (PEPT), a non-invasive method, was used to track a single tracer particle [34]. From the results, distributions of residence times of the solids were calculated, where a single residence time was defined as the time, experimentally, that the tracer particle spent within the defined boundaries of the air and fuel reactors. The relevant volumes are shown in Fig. 14 in Appendix A. Although theoretically possible, it was not observed that the tracer re-entered the reactors after initially leaving.

The tracer particle was a gamma-alumina substitute for a sand particle of similar density, size and shape as the silica sand particles used in the CFB. The tracer particle was labelled with the proton-rich radionuclide ^{18}F (half-life ~ 110 min), which undergoes beta-decay, accompanied by the emission of positrons. Upon contact with an electron, annihilation occurs, resulting in the emission of a pair of back-to-back ($180° \pm 0.5°$) gamma-rays of 511 keV each. An ADAC Forte dual-headed gamma camera was used to detect these coincident gamma rays to locate the tracer particle. The x-, y- and z-coordinates of the particle were obtained as a function of time, with the absolute error associated with each position being no more than 7 mm.

It was found that, although the mean residence time of particles changed when the circulation rate of solids, $\dot{m}_s$, was altered, the shape of the RTD remained almost the same, within the limits investigated [35]. Typical RTDs for the air and fuel reactors are shown in Fig. 8 ($\dot{m}_s = 3.7$ g/s and $\dot{m}_s = 5.9$ g/s for the air and fuel reactor respectively). The mean residence time and the standard deviation of the RTDs were calculated from the experimental measurements, and using Eq. (5), the equivalent number of tanks in series, N was calculated. The values are given in Table 1. The values of N calculated were used as inputs for tanks-in-series with gamma extension models for the air and fuel reactors. The resulting model RTDs are also shown in Fig. 8. Given the restricted number of data points, chi-squared goodness of fit tests were used to determine confidence intervals on N for the air and fuel reactors. The tests showed that the experimental data can be modelled satisfactorily at the 5% level, with N in the range 0.8–2.5 for the air reactor and 0.5–1.5 for the fuel reactor. The results indicate that the hydrodynamics in the two reactors are unlikely to be the same, probably due to differences in geometry. The fuel reactor can be assumed to be well-mixed with respect to solids. While this would be within the confidence interval on N for the air reactor, it is at the extreme lower end.

Two simulations were run to assess whether a TIS with gamma extension model is appropriate for modelling experimental RTDs. In the first, the experimental RTDs were used in the MC simulation i.e. the rejection sampling algorithm was used to sample directly from the experimental RTDs shown in Fig. 8. In the second simulation, the values of N, given in Table 1 ($N = 1.08$ and $N = 1.51$ for the fuel and air reactors respectively) were used as parameters for the TIS with gamma extension model. In Fig. 9, the results for the mean conversion of particles as they leave the reactors are shown for both simulations. It is clear that there is excellent agreement for all values of θ.

In Fig. 10, the results for the mean rate of reaction of particles in the reactors are shown for both simulations. As for the case of the mean conversion of particles as they leave the reactors, there is excellent agreement for all values of θ.
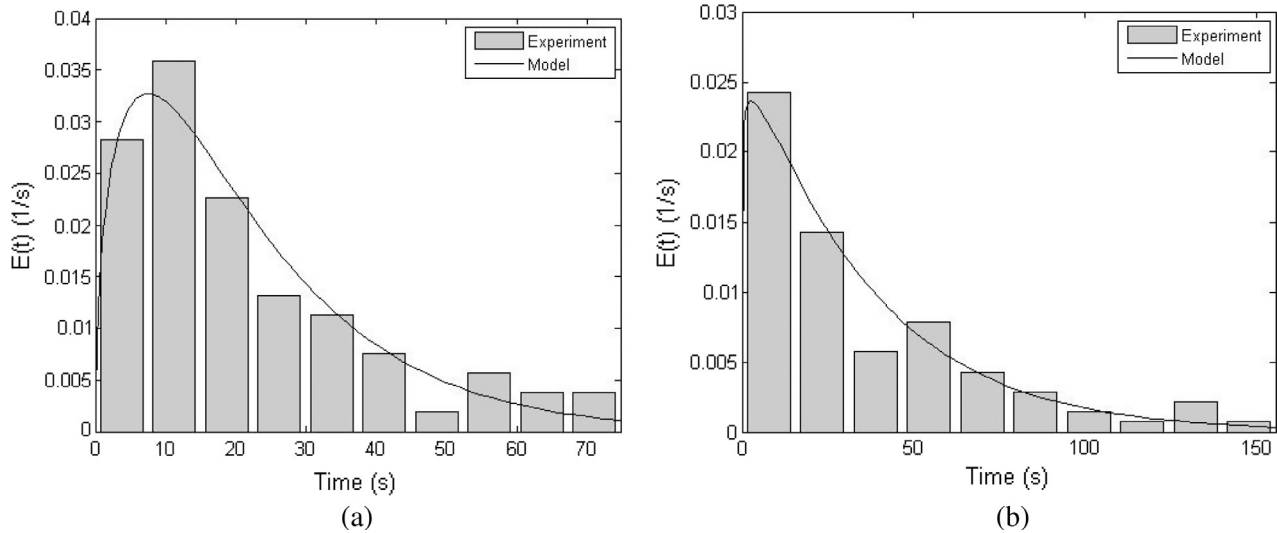
Fig. 8. RTDs for a laboratory-scale CFB, determined from positron emission particle tracking data [35] and the model fit using the values of N from Table 1 in a tanks-in-series with gamma extension model, (a) is for the air reactor and (b) for the fuel reactor.

Table 1
The mean residence times, standard deviation and the equivalent number of tanks-in-series for the RTDs from a laboratory-scale CFB [35].

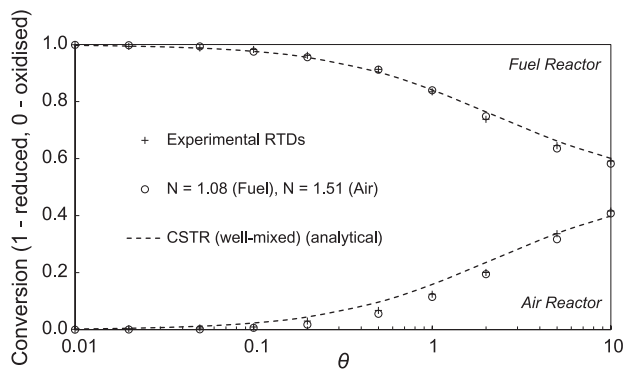|	Number of data points	Mean residence time, $\bar{t}$ (s)	Standard deviation, σ (s)	N
Fuel reactor	90	36.0	34.7	1.08
Air reactor	71	22.2	18.1	1.51

Fig. 9. Mean conversions of particles as they leave the reactors, using the experimental RTDs, shown in Fig. 8, and using the calculated values of N for the laboratory-scale CFB in a TIS with gamma extension model ($N = 1.08$ and $N = 1.51$ for the fuel and air reactors respectively). The analytical solution when the two reactors are well-mixed is also shown.

3.3. The effect of different mixing in the air and fuel reactors

The degree of mixing and therefore the value of N will not necessarily be the same in both reactors of a coupled system, as demonstrated in Section 3.2. Further simulations were run where the mixing in one of the reactors (the fuel reactor) was kept constant at $N = 1$, while that in the air reactor was varied ($N = 2$, 5 and 50). In Fig. 11, the mean conversions of particles as they leave the reactors is shown for these different cases. The mean rate of reaction of particles in the reactors is shown in Fig. 12 and Fig. 13 for the fuel and air reactors respectively. The second simulation result from Section 3.2 is also shown, with values of N determined for the laboratory-scale CFB (given in Table 1). These results are also shown in Figs. 11–13.

In Fig. 9, whilst an increase in the value of N leads to a significant shift in the mean conversion of particles as they leave the reactors, the increase in the important parameter, ΔX is far less significant than
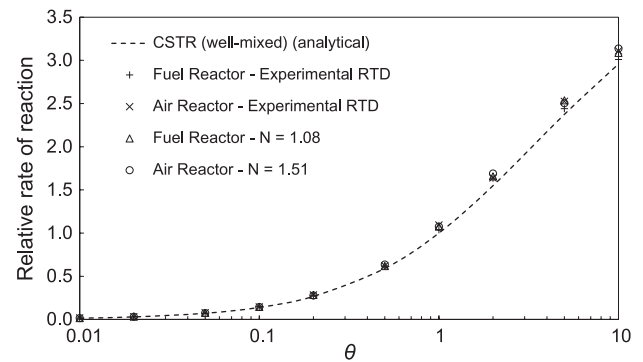

Fig. 10. Mean rate of reaction of particles in the fuel and air reactors, using the experimental RTDs, shown in Fig. 8, and using the calculated values of N for the laboratory-scale CFB in a TIS with gamma extension model ($N = 1.08$ and $N = 1.51$ for the fuel and air reactors respectively). The analytical solution when the two reactors are well-mixed is also shown. The rate values are relative to the well-mixed value when $\theta = 1$.
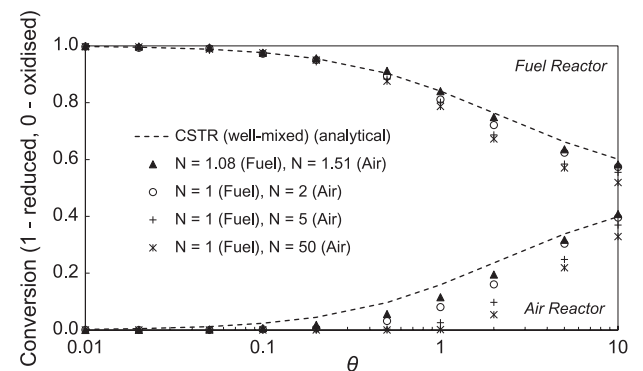

Fig. 11. Mean conversions of particles as they leave the reactors as the RTD in the air reactor is varied. The results using the calculated values of N for the laboratory-scale CFB are also shown.

when N in both reactors is increased. For $\theta = 1$, an increase in the value of N in both reactors from 1 to 2 raises ΔX from 0.682 to 0.824 (Fig. 3), while when N is increased in the air reactor only from 1 to 2, ΔX rises to 0.731 (Fig. 11). The mean rate of reaction in the beds also increases much less significantly when only the mixing in the air reactor is changed (Figs. 12 and 13). The trends are exactly the same when N is kept constant in the air reactor and varied in the fuel reactor. As
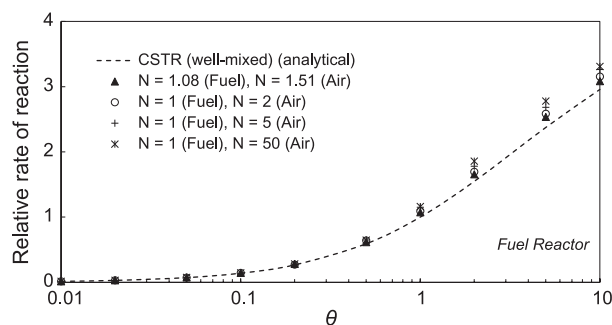
Fig. 12. Mean rate of reaction of particles in the fuel reactor as the RTD in the air reactor is varied. The result using the calculated values of N for the laboratory-scale CFB are also shown. The rate values are relative to the well-mixed value when $\theta = 1$.

Fig. 13. Mean rate of reaction of particles in the air reactor as the RTD in the air reactor is varied. The result using the calculated values of N for the laboratory-scale CFB are also shown. The rate values are relative to the well-mixed value when $\theta = 1$.
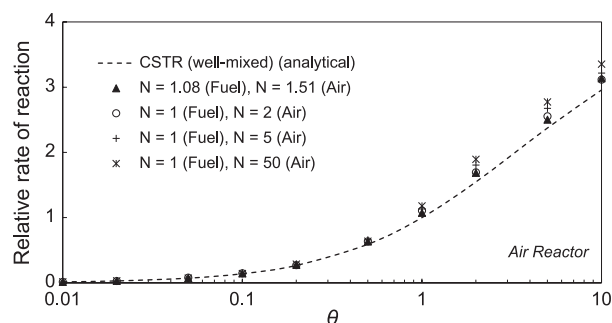
expected, the results from the simulation using the values of N determined for the laboratory-scale CFB lie between the well-mixed result and that when $N = 1$ in the fuel reactor and $N = 2$ in the air reactor.

4. Discussion

CLC is likely to be operated in an interconnected fluidised bed arrangement [36]. Figs. 3 and 11 show that the mean conversion of particles as they leave the reactors is sensitive to different RTDs in the air and fuel reactors when $\theta > 0.1$, i.e. when the mean residence time of particles is less than ten times the characteristic time taken for a particle to react completely. When operated in this regime, an increase in the number of CSTRs, N, corresponding to a decrease in the degree of mixing of the particles, was found to increase $\Delta X = X_{fuel} - X_{air}$. The impact is greatest around $\theta = 1$. This is the region where CLC is likely to be operated, since it gives the optimal balance between a low circulation rate and low inventories of solids, as seen in Fig. 7. ΔX is an important parameter since it has an impact on the amount of lattice oxygen transferred from the air to the fuel reactor each time a particle is cycled. In terms of the mean rate of reaction of particles in the beds, CLC was found to be sensitive to the extent of mixing when $\theta > 0.5$, as concluded from Figs. 5, 12 and 13. At higher values of θ, a decrease in mixing led to an increase in the mean rate of reaction. This is because a smaller degree of mixing means that it is less likely that any given particle will have sufficient time to react completely, since the spread of residence times decreases. Decreasing the mixing in only one of the reactors led to significantly smaller increases in ΔX and mean rate of reaction in the beds, as shown in Figs. 11–13.

The fact that a decrease in the extent of mixing in the fluidised beds, for the same value of θ, results in a greater ΔX and a higher mean rate of reaction is valuable for design. A reduction in the mixing should therefore allow the size of the CLC system to be decreased because a lower solid circulation rate and a lower inventory of solids will be required for the same combustion performance. For example, consider a

particle reacting according to a SCM under chemical reaction control, and being used in CLC, operating with $\theta = 1$ in both reactors. If the value of N in both reactors were increased from 1 to 2, ΔX would rise from 0.6822 to 0.8242, as seen in Fig. 3, and the mean rate of reaction in the beds would increase by 37%, as seen in Fig. 5. In this case, the solid circulation rate could be decreased by around 18% and the inventory by 17%, as seen in Fig. 7, representing considerable savings in capital and operating expenditure. Increasing N in only one of the reactors is also beneficial, but the effect is far less pronounced, as illustrated in Fig. 11. Porrazzo et al. [37] estimated that the cost of the CLC reactors accounts for 64% of the capital cost of a natural gas combined cycle power plant with CLC technology. Therefore considerable savings in capital expenditure are achievable by modifying the RTD of particles in the two reactors. Savings in operating expenditure are also achievable.

As the degree of mixing is reduced, Fig. 4 shows that the spread of conversion in particles leaving the reactors decreases, making it possible to have tighter control on X_{air} and X_{fuel}. This could be useful, for example, if coking of the oxygen carrier particles were a problem in the fuel reactor at high X_{fuel} [38,39]. In this case it might be desirable to set a limit on the degree of reduction. Alternatively, it might be the case that if a particle were highly reduced in the fuel reactor it might result in an excessive temperature rise upon re-oxidation in the air reactor. This occurrence could lead to significant sintering and degradation of the particle each time it happens. In this case, it would also be desirable to control the degree of reduction of particles.

The spread in the values of rates of reaction in the bed with respect to θ and the RTDs of particles in the reactors is interesting. For $\theta < 1$, the spread is the same regardless of the mixing behaviour, as seen in Fig. 6, and increases linearly with θ. This is because the proportion of particles in the bed that have reacted to completion decreases. As θ increases beyond 1, especially when there is a small degree of mixing (e.g. $N = 50$), the likelihood that a particle will react to completion decreases. For this reason the spread of rates decreases again and is lower when there is a smaller degree of mixing.

Physically, the RTD of solids in fluidised beds can be modified by altering the design or the operation of the reactor. In the bubbling regime, bubbles lead to good mixing of the solids and beds are generally well-mixed with respect to solids [22]. In terms of operation, increasing the superficial gas velocity or decreasing the solid circulation rate, leads to better mixing in bubbling beds [21,27]. In the fast fluidisation regime, an increase in the superficial gas velocity or a decrease in the solid circulation rate decreases the mean residence time of solids, decreases the variance and increases the coefficient of variation [40]. A change in the geometry of the bed, e.g. by the addition of baffles, by modification of the aspect ratio, by adding stages, or by modifying the exit has been found to alter the mixing behaviour [21,23,41]. Increasing the size of particles can lead to a reduction in mixing [42,43]. Of course, the RTDs of solids could be changed dramatically by switching to a different type of reactor e.g. from a fluidised bed to a moving bed [44].

The mean and standard deviations of experimental RTDs from a laboratory-scale CFB gave values of N close to 1, as seen in Table 1. Fig. 9 and Fig. 10 show that modelling experimental RTDs using a TIS with gamma extension model is an excellent approximation. In fact Fig. 11 shows that the difference between the mean conversion of particles as they leave the reactors when assuming that the reactors are well-mixed (the analytical solution) and when the appropriate values of N ($N = 1.08$ in the fuel reactor and $N = 1.51$ in the air reactor) were used was small. The difference between using the later and using values of $N = 1$ and $N = 2$ for the fuel and air reactors respectively was also small. The same trend was seen for the mean rates of reaction in the beds, shown in Figs. 12 and 13.

Generating RTDs of solids for laboratory and industrial CFBs is challenging, expensive and time-consuming. This work indicates that for $N \leq 5$, knowing N to at least the nearest integer is important for
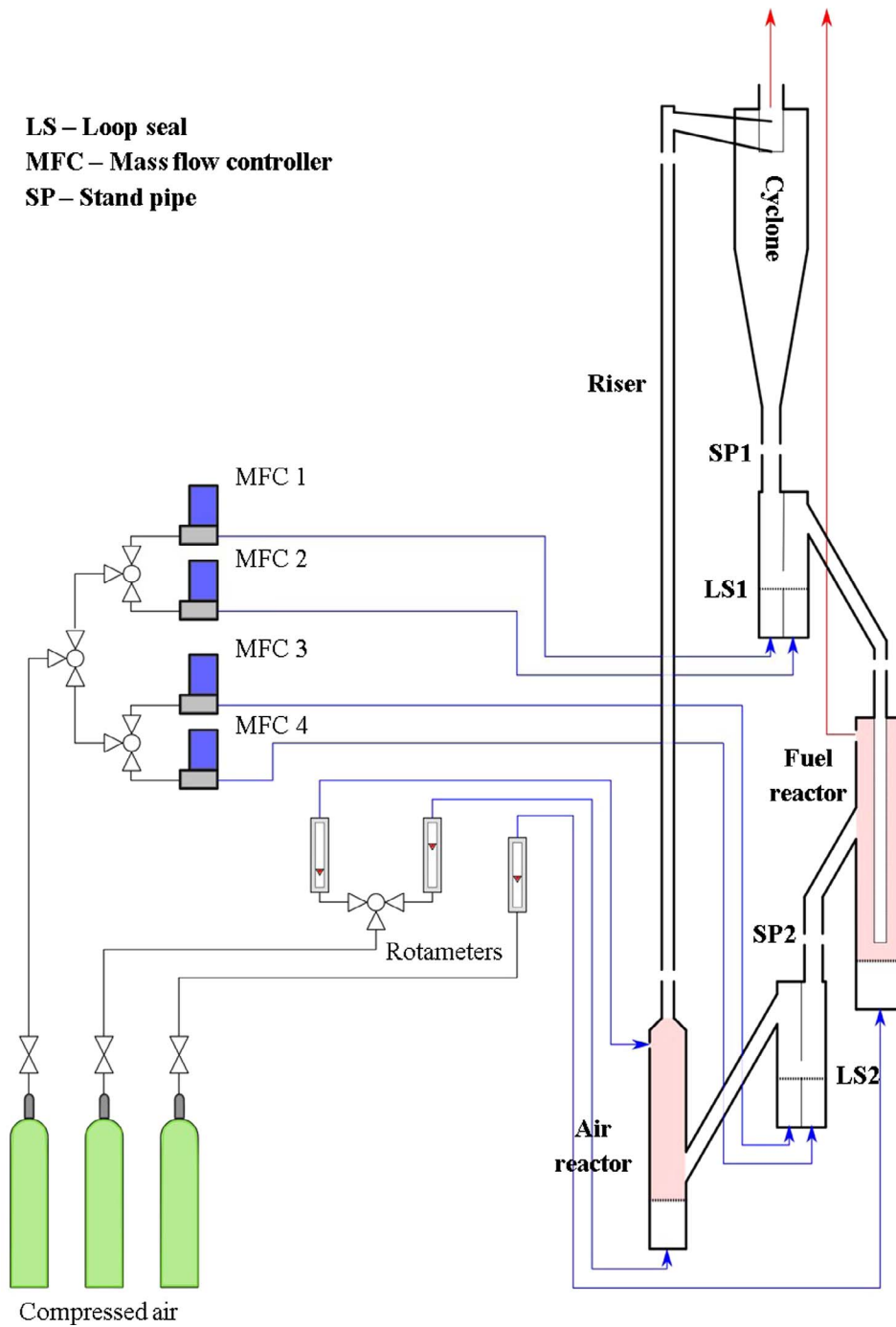
Fig. 14. Schematic diagram of the experimental CFB. The shaded regions indicate the volumes relevant for measurement of the RTDs using a single tracer particle.

generating accurate models at the reactor scale. As N increases, the sensitivity of the coupled system decreases, so for $N > 5$, knowing the value to the nearest 5 or 10 tanks is sufficient. These criteria are valid whether N is the same or different in the two reactors.

5. Conclusions

The sensitivity of CLC to different RTDs of solids in the air and fuel reactors has been investigated. It was found that when the mean residence time of particles is less than ten times the characteristic time taken for a particle to react completely, CLC is sensitive to different RTDs. A decrease in the extent of mixing leads to a greater mean conversion by the time the particles leave the reactors, meaning that more oxygen is transferred each time a particle is cycled. It also leads to

greater mean rates of reaction in the beds, allowing the inventory and circulation rate of solids to be lowered for the same combustion performance. This is valuable for design since it could significantly reduce the capital and operating costs of a CLC process. It was found that, for the case of a laboratory-scale CFB, described in this paper, it is appropriate to assume that both reactors are well-mixed with respect to solids. Generally in design and modelling of the CLC process it is important to take account of the residence time distribution of solids. If a tanks-in-series approach is used, for small values of N, knowing N to the nearest integer is likely to be sufficient, while for higher values, to the nearest 5 or 10 tanks is sufficient.

Appendix A. Description of laboratory-scale circulating fluidised bed

Fig. 14 shows a schematic diagram of the experimental CFB, which was made of stainless steel (Alloy 310) and consisted of two fluidised bed reactors connected through two identical loop seals. The fuel reactor (FR) was a bubbling fluidised bed with an operating bed height of ~100 mm and an i.d. of 40 mm. The solids were transported from the FR to the air reactor (AR) *via* the lower standpipe (SP2) and the lower loop seal (LS2). The loop seals consisted of two chambers, which could be aerated independently. They each had a cross-sectional area of 20 mm × 20 mm and a height of 80 mm. The AR was a bubbling fluidised bed with an operating bed height of ~120 mm and an i.d. of 27 mm. The outlet of the AR tapered to a tube with a length ~1.6 m and an i.d. of 10 mm, acting as a riser to transport the solids upwards. To assist with the transport of particles up the riser, secondary air could be injected at the top of the bubbling fluidised bed of the AR. The solids were recovered downstream of the riser by a cyclone and transported *via* the upper standpipe (SP1) to the upper loop seal (LS1). Particles from LS1 entered the FR *via* tubing of i.d. 10 mm. This tubing was immersed in the bed of the FR, with the exit 15 mm above the distributor. The standpipes were operated in packed bed flow.

The pressure drop across various sections of the CFB was monitored continuously (at a frequency of 10 Hz) using pressure transducers (First Sensor, HDI) to ensure the system operated stably. Mass flow controllers (Brooks, 5850S) were used to control the flow rate of air to the LSs. Rotameters (MPB Industries) were used to control the flow rates of air to the AR (primary and secondary air inlet) and to the FR.

The circulation rate of solids, $\dot{m}_s$, was measured in the riser of the CFB, using a method developed and validated for this system. This is described in detail elsewhere [35]. In brief, pressure signals associated with the passage of solids in the riser were cross-correlated to estimate their time-averaged velocity, U_p. At the same time, the time-averaged voidage, ε_{riser}, was measured in the riser. This enabled the value of $\dot{m}_s$ to be computed using $\dot{m}_s = A_{riser} \times \rho_p \times (1 - \varepsilon_{riser}) \times U_p$, where A_{riser} is the cross-sectional area of the riser and ρ_p is the particle density.

References

[1] Chen Y-M. Applications for fluid catalytic cracking. In: Yang W-C, editor. Handb fluid fluid-particle syst. New York: Marcel Dekker; 2003. p. 385–402.

[2] Adanez J, Abad A, Garcia-Labiano F, Gayan P, de Diego LF. Progress in chemical-looping combustion and reforming technologies. Prog Energy Combust Sci 2012;38:215–82. http://dx.doi.org/10.1016/j.pecs.2011.09.001.

[3] Adánez J, Abad a, Mendiara T, Gayán P, de Diego LF, García-Labiano F. Chemical looping combustion of solid fuels. Prog Energy Combust Sci 2017. http://dx.doi.org/10.1016/j.pecs.2017.07.005.

[4] Imtiaz Q, Hosseini D, Müller C. Review of oxygen carriers for chemical looping with oxygen uncoupling (CLOU): thermodynamics, material development, and synthesis. Energy Technol 2013;1:633–47. http://dx.doi.org/10.1002/ente.201300099.

[5] Spallina V, Hamers HP, Gallucci F, van Sint Annaland M. Chemical Looping Combustion for Power Production. In: Gallucci F, van Sint Annaland M, editors. Process intensif sustain energy convers, Chichester, UK: John Wiley & Sons; 2015, p. 117–74.

[6] Ströhle J, Orth M, Epple B. Design and operation of a 1MWth chemical looping plant. Appl Energy 2014;113:1490–5. http://dx.doi.org/10.1016/j.apenergy.2013.09.008.

[7] Abad A, Pérez-Vega R, de Diego LF, García-Labiano F, Gayán P, Adánez J. Design and operation of a 50 kWth Chemical Looping Combustion (CLC) unit for solid fuels. Appl Energy 2015;157:295–303. http://dx.doi.org/10.1016/j.apenergy.2015.03.094.

[8] Andrus, H., Chui, J., Thibeault, P., Edberg, C., Turke, D., Kenney, J., Abdullay, I., Chapman, P., Kang S. Alstom's limestone-based (LCL) chemical looping process. In": 2nd int conf chem looping. TU Darmstadt, Ger., 2012.

[9] Markström P, Linderholm C, Lyngfelt A. Operation of a 100kW chemical-looping combustor with Mexican petroleum coke and Cerrejón coal. Appl Energy 2014;113:1830–5. http://dx.doi.org/10.1016/j.apenergy.2013.04.066.

[10] Markström P, Berguerand N, Lyngfelt A. The application of a multistage-bed model for residence-time analysis in chemical-looping combustion of solid fuel. Chem Eng Sci 2010;65:5055–66. http://dx.doi.org/10.1016/j.ces.2010.06.029.

[11] Abad A, Gayán P, de, Diego LF, García-Labiano F, Adánez J. Fuel reactor modelling in chemical-looping combustion of coal: 1. model formulation. Chem Eng Sci 2013;87:277–93. http://dx.doi.org/10.1016/j.ces.2012.10.006.

[12] Parker JM. CFD model for the simulation of chemical looping combustion. Powder Technol 2014;265:47–53. http://dx.doi.org/10.1016/j.powtec.2014.01.027.

[13] Porrazzo R, White G, Ocone R. Fuel reactor modelling for chemical looping combustion: from micro-scale to macro-scale. Fuel 2016;175:87–98. http://dx.doi.org/10.1016/j.fuel.2016.01.041.

[14] Guan Y, Chang J, Zhang K, Wang B, Sun Q. Three-dimensional CFD simulation of hydrodynamics in an interconnected fluidized bed for chemical looping combustion. Powder Technol 2014;268:316–28. http://dx.doi.org/10.1016/j.powtec.2014.08.046.

[15] Mahalatkar K, Kuhlman J, Huckaby ED, O'Brien T. CFD simulation of a chemical-looping fuel reactor utilizing solid fuel. Chem Eng Sci 2011;66:3617–27. http://dx.doi.org/10.1016/j.ces.2011.04.025.

[16] Cuadrat A, Abad A, Gayán P, De Diego LF, García-Labiano F, Adánez J. Theoretical approach on the CLC performance with solid fuels: optimizing the solids inventory. Fuel 2012;97:536–51. http://dx.doi.org/10.1016/j.fuel.2012.01.071.

[17] Zhang Y, Chao Z, Jakobsen Ha. Modelling and simulation of chemical looping combustion process in a double loop circulating fluidized bed reactor. Chem Eng J 2017;320:271–82. http://dx.doi.org/10.1016/j.cej.2017.03.046.

[18] Ohlemüller P, Alobaid F, Gunnarsson A, Ströhle J, Epple B. Development of a process model for coal chemical looping combustion and validation against 100 kWth tests. Appl Energy 2015;157:433–48. http://dx.doi.org/10.1016/j.apenergy.2015.05.088.

[19] Levenspiel O. Chemical reaction engineering. New York: Wiley; 1999.

[20] Froment GF, Bischoff KB, De Wilde J. Chemical reactor analysis and design. 3rd ed. New York: John Wiley & Sons; 2011. 10.1017/CBO9781107415324.004.

[21] Kunii D, Levenspiel O. Fluidization engineering. New York: John Wiley & Sons; 1977.

[22] Yang W-C, editor. Handbook of fluidization and fluid-particles systems New York: Marcel Dekker, Inc; 2003. http://dx.doi.org/10.1016/S1672-2515(07)60126-2.

[23] Werther J. Fluidized bed reactors. Ullmann's encycl indusitrial chem, Weinheim, Germany: John Wiley & Sons; 2012, p. 320–66. http://doi.org/10.1002/14356007.b04.

[24] Markström P. Design, modelling and operation of a 100 kW chemical-looping combustor for solid fuels; 2012.

[25] Guío-Pérez DC, Pröll T, Hofbauer H. Influence of ring-type internals on the solids residence time distribution in the fuel reactor of a dual circulating fluidized bed system for chemical looping combustion. Chem Eng Res Des 2014;92:1107–18. http://dx.doi.org/10.1016/j.cherd.2013.10.018.

[26] Guío-Pérez DC, Pröll T, Hofbauer H. Solids residence time distribution in the secondary reactor of a dual circulating fluidized bed system. Chem Eng Sci 2013;104:269–84. http://dx.doi.org/10.1016/j.ces.2013.08.047.

[27] Babu MP, Setty YP. Residence time distribution of solids in a fluidized bed. Can J Chem Eng 2003;81:118–23. http://dx.doi.org/10.1002/cjce.5450810114.

[28] Rao JS, Ramani NVS, Pant HJ, Reddy DN. Measurement of residence time distributions of coal particles in a pressurized fluidized bed gasifier (PFBG) using radio tracer technique. Indian J Sci Technol 2012;5:3746–52.

[29] Nauman EB, Buffham BA. Mixing in continuous flow systems. New York: Wiley-VCH; 1983.

[30] Buffham BA, Gibilaro LG. A generalization of the tanks-in-series mixing model. AIChE J 1968;14:805–6.

[31] Schnellmann MA, Scott SA, Williams G, Dennis JS. Sensitivity of chemical-looping combustion to particle reaction kinetics. Chem Eng Sci 2016;152:21–5. http://dx.doi.org/10.1016/j.ces.2016.05.028.

[32] Kimura S, Fitzgerald J, Levenspiel O, Kottman C. Solid circulation systems with shrinking core kinetics in both reactor and regenerator. Chem Eng Sci 1979;34:1195–201.

[33] Donat F, Hu W, Scott Sa, Dennis JS. Use of a chemical-looping reaction to determine the residence time distribution of solids in a circulating fluidized bed. Energy Technol 2016;4:1230–6. http://dx.doi.org/10.1002/ente.201600140.

[34] Parker DJ, Broadbent CJ, Fowles P, Hawkesworth MR, McNeil P. Positron emission particle tracking – a technique for studying flow within engineering equipment. Nucl Inst Methods Phys Res A 1993;326:592–607. http://dx.doi.org/10.1016/0168-9002(93)90864-E.

[35] Donat F. Development of a laboratory-scale system for chemical looping combustion. University of Cambridge; 2016.

[36] Lyngfelt A, Leckner B, Mattisson T. A fluidized-bed combustion process with inherent CO2 separation; application of chemical-looping combustion. Chem Eng Sci 2001;56:3101–13.

[37] Porrazzo R, White G, Ocone R. Techno-economic investigation of a chemical

looping combustion based power plant. Faraday Discuss 2016.

[38] Chuang SY. Development and performance of a Cu-based combustion of solid fuels. University of Cambridge; 2009.

[39] De Diego LF, Gayán P, García-Labiano F, Celaya J, Abad A, Adánez J. Impregnated CuO/Al$_2$O$_3$ oxygen carriers for chemical-looping combustion: avoiding fluidized bed agglomeration. Energy Fuels 2005;19:1850–6. http://dx.doi.org/10.1021/ef050052f.

[40] Harris AT, Davidson JF, Thorpe RB. Particle residence time distributions in circulating fluidised beds. Chem Eng Sci 2003;58:2181–202. http://dx.doi.org/10.1016/S0009-2509(03)00082-4.

[41] Harris AT, Davidson JF, Thorpe RB. The influence of the riser exit on the particle residence time distribution in a circulating fluidised bed riser. Chem Eng Sci 2003;58:3669–80. http://dx.doi.org/10.1016/S0009-2509(03)00215-X.

[42] Burovoi IA, Svetozarova GI. Determination of the mixing coefficient in a fluidized bed reactor. Int Chem Eng 1965;5:711–9.

[43] Patience GS, Chaouki J, Kennedy G. Solids residence time distribution in CFB reactors. In: Basu P, Horio M, Hasatani M, editors. Circ Fluid Bed Technol III, Oxford: Pergamon; 1991, p. 599–604.

[44] Tong A, Bayham S, Kathe MV, Zeng L, Luo S, Fan LS. Iron-based syngas chemical looping process and coal-direct chemical looping process development at Ohio State University. Appl Energy 2014;113:1836–45.